

Development of a New Type Snow Fence with Airfoil Snow Plates to Prevent Blowing-Snow Disasters: Part 2, Characteristics of the Aerodynamic Fluid Forces of Airfoil Snow Plates

Hiroshi SAKAMOTO

Professor, Kitami Institute of Technology

Masaru MORIYA

Associate Professor, Kitami Institute of Technology

Kazunori TAKAI

Research Scientist, Kitami Institute of Technology

Yoshihiro OBATA

Research Scientist, Kitami Institute of Technology

(Received for 12 Jul., 2000 and in revised from 9 May., 2001)

ABSTRACT

A new snow fence with airfoil snow plates was developed to prevent blowing-snow disasters. In a previous report, we showed that in comparison with the conventional snow fence, this snow fence with airfoil snow plates performed very well in preventing snowdrifts and in improving visibility. The characteristics of the aerodynamic fluid forces on and flow-induced vibrations of the airfoil snow plates now have been investigated. The important findings are (i) fluctuating fluid forces acting on the airfoil snow plate set at the topmost part of the snow fence are the most serious, (ii) flow-induced vibrations generated in the airfoil snow plate attached to the topmost part of the snow fence are rapidly amplified by an increase in wind velocity, (iii) the fluctuating fluid forces on and flow-induced vibrations in the airfoil snow plates could be completely suppressed when a perforated plate was attached to the topmost part of the snow fence.

1. INTRODUCTION

Most traffic difficulties on winter roads are caused by the formation of snowdrifts and visibility blockage generated by blowing snow. Blow-off type snow fences are commonly used as a countermeasure of road transportation disasters being caused by blowing snow. In a previous report (Sakamoto et al. 2001), a snow fence was developed that has airfoil snow plates, whose shape differs completely from that of the flat snow plates used for conventional snow fences. Examinations based on results of blowing-snow simulation tests in a wind tunnel showed that the newly developed snow fence had high performance and was sufficient for use on a road 20 m wide. The aerodynamic characteristics of the newly developed snow fence with airfoil snow plates were investigated and the findings are discussed here. Little research on the aerodynamic characteristic of snow fence has been studied, only that which examined time-averaged fluid forces (Sakamoto et al. 1992). Because lightening of the weight of snow plates which constitute a snow fence is desirable, it is necessary to understand the unsteady aerodynamic forces acting on and characteristics of the flow-induced vibration of these snow plates. We therefore have studied in detail the unsteady aerodynamic fluid forces that cause fatigue breakdown in airfoil snow plates. The response characteristics of airfoil snow plates generated by flow-induced vibration also were investigated by the use of a free vibration model test

in a wind tunnel. A method for the suppression of unsteady aerodynamic fluid forces and flow-induced vibrations by means of a perforated plate attached to the topmost part of the snow fence is presented, and its effectiveness verified.

2. EXPERIMENTAL ARRANGEMENT AND PROCEDURES

The aerodynamic fluid forces acting on the snow fence and the airfoil snow plates were measured in a low-speed, closed-circuit wind tunnel. The test section of the wind tunnel was 0.3×1.2 m in cross section and 2.5 m in long. Time-averaged fluid forces (steady fluid forces) and fluctuating fluid forces (unsteady fluid forces) were measured in box-type load cells. The time-averaged fluid forces acting on the snow fence, necessary for evaluating the required strength of the support and installed base size of the snow fence, were measured for a single load cell, (Fig.1 (a)). These fluid forces that act on airfoil snow plates also were measured for two load cells that had identical characteristics. The two load cells attached to double sides of the snow plate were used (Fig.1 (b)), to raise the natural frequency of the snow plate as much as possible. The natural frequency, f_n , of the airfoil snow plate supported by the two load cells was 400 Hz, about 20 times the prevailing frequency (19.9 Hz) of the fluctuating fluid forces. Fluctuating fluid forces therefore could be measured with sufficient accuracy (So et al. 1981). A snow fence with Joukowsky airfoil snow plates also was

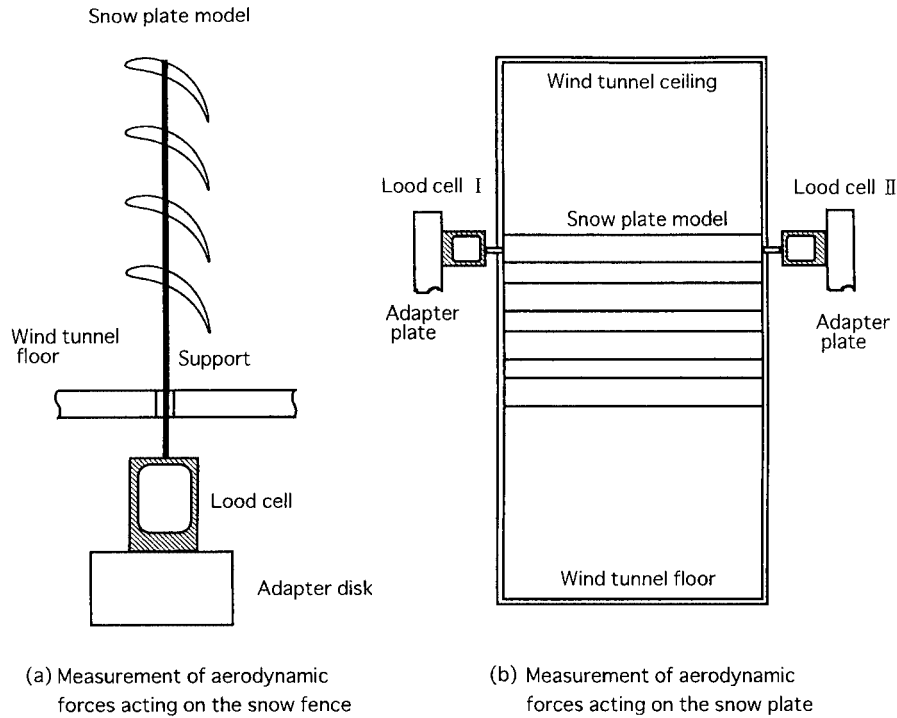


Fig. 1 Load cell apparatus for measuring of aerodynamic force acting on the snow fence and snow plates

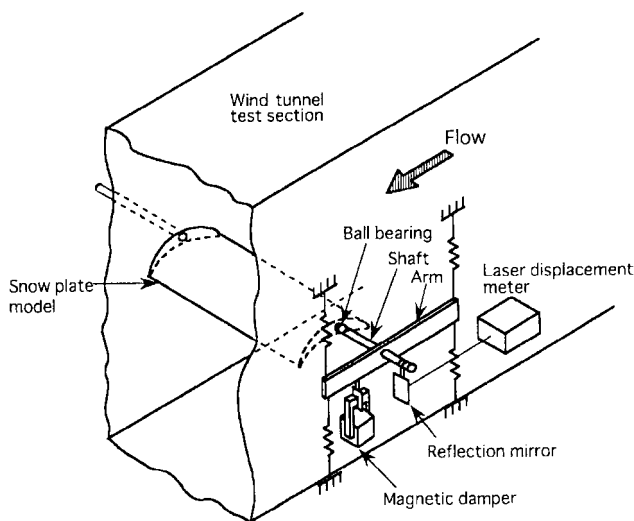


Fig. 2 Schematic diagram of the free-vibration apparatus

tested. The fence height was $H=2.8$ m, the bottom gap $K=1.2$ m, snow plate size $W=650$ mm and setup angle of the snow plate $\beta=60^\circ$ the dimensions that gave the best performance in a previous report. The airfoil snow plate was constructed of wood to reduce its weight as much as possible. In the experiment, the free-stream velocity was kept constant at 9 m/s. The model snow fence tested was 1/15.5 the size of the prototype. The corresponding Reynolds number, R_n , was 1.04×10^5 .

The flow-induced vibrations of the airfoil snow plate were evaluated with the free-vibration equipment shown in Fig.2. There are two modes of flow-induced vibration; cross-flow and rotational vibration of the airfoil snow plate. In this study, we found rota-

tional vibration, and examined the response characteristics. The airfoil snow plate was constructed of balsawood to make the model as light as possible. A rotating shaft installed in two bearings attached to each side wall of the wind tunnel was supported by four coil springs installed in the arms to allow free rotational oscillation. Displacement of rotational oscillation was measured with a laser displacement meter. The reduced velocity, $U_r [=U/(f_c \cdot W)]$ varied in the range of 0–16. The natural frequency, f_c , of the airfoil snow plate installed on the free-vibration equipment was 9 Hz. In addition, the reduced damping factor, $C_n [=I \delta / (\rho W^4)]$, in which I is the inertia moment of the airfoil snow plate and δ the logarithmic damping factor, was 0.0046.

Next, the fluctuating fluid forces and flow-induced vibrations of the airfoil snow plates were suppressed by means of a perforated plate attached to the topmost part of the snow fence (Fig.3). In this experiment, the width, w , of the perforated plate was kept constant, and the porosity, a , and interval between the topmost snow plate and the perforated plate, G , were varied. The model snow fence tested was 1/5.4 the size of the prototype.

3. RESULTS AND DISCUSSIONS

3.1 Time-averaged aerodynamic fluid forces acting on the snow fence

Figures 4 and 5 respectively show the time-averaged drag coefficient, C_{DH} , and time-averaged lift coefficient, C_{LH} , of the newly developed snow fence for changes in the setup angle, β , of the airfoil snow plates in the range of 10° – 80° . C_{DH} and C_{LH} are defined by:

$$(C_{DH}, C_{LH}) = (D_H, L_H) / (0.5 \rho U^2 A) \quad (1)$$

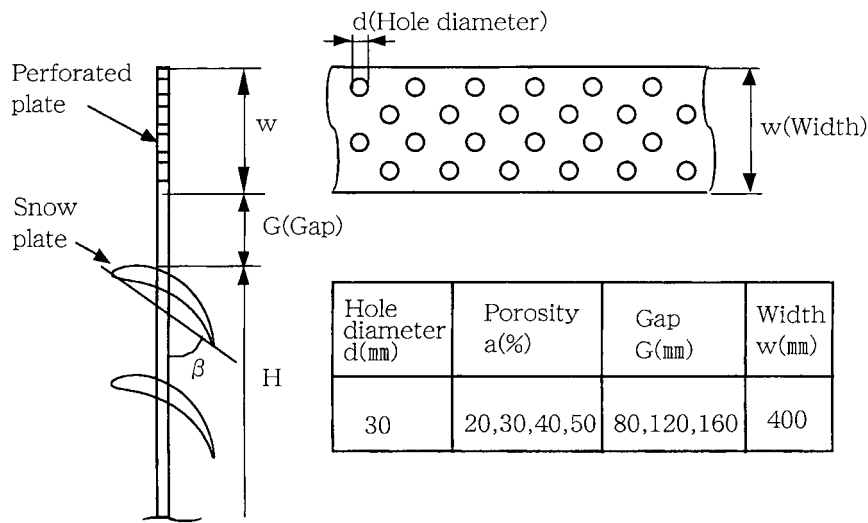


Fig. 3 Perforated plate for snow flow control

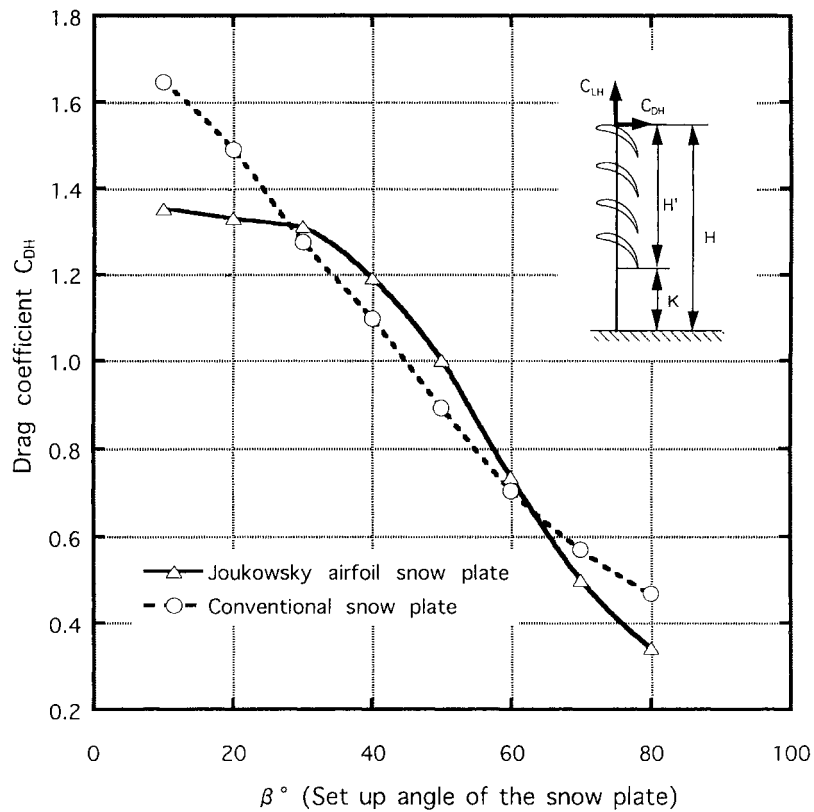


Fig. 4 Drag coefficient, C_{DH} , of the snow fence versus the set up angle, β

Where D_H and L_H respectively are the time-averaged drag and the time-averaged lift, and A is the projected area $A=H' \times l$ (in which H' is the height of the snow fence, H , minus the bottom gap height of K , and l the length of the span of the snow fence). C_{DH} and C_{LH} for a conventional snow fence are shown in these figures for comparison. C_{DH} decreases as setup angle β of the airfoil snow plate increases, because flow blockage through the snow plates decreases as the setup angle increases. Also, C_{DH} in the case of $\beta = 60^\circ$ of the snow plate in the previous report for which the blow-

ing-off effect was highest is about 0.75. This value is considerably smaller than $C_{DH} = 1.30$ for a conventional snow fence with flat snow plates and an optimum setup angle of $\beta = 23.5^\circ$. The wake formed behind the newly developed snow fence therefore is considerably reduced compared to that formed behind the conventional snow fence. The time-averaged lift coefficient, C_{LH} , increases as setup angle β of the airfoil snow plate increases, reaching a maximum at the optimum angle $\beta = 60^\circ$ because separation of the flow passing through the snow plate is suppressed the most at that

angle.

Figure 6 shows the time-averaged fluid forces acting on the airfoil snow plates. The time-averaged drag coefficient, C_D , lift coefficient, C_L , and resultant force coefficient, C_R , are defined by :

$$(C_D, C_L) = (D, L) / (0.5 \rho U^2 Wl) \tag{2}$$

$$C_R = \sqrt{C_D^2 + C_L^2}$$

Where, D is the force in the flow direction, L the force in the direction perpendicular to the flow, and C_D and C_L are the maximum values for the airfoil snow plate of ②. This is because the deflection of the flow passing through the snow plate of ② becomes large, as seen from the visualized observations shown in Fig.10. It therefore is necessary to evaluate the required strength of the airfoil snow plate of ② based on aerodynamic forces.

3.2 Fluctuating drag and lift acting on snow plates

Figure 7 shows the fluctuating drag, C_{Df} and fluctuating lift coefficient, C_{Lf} , for each airfoil snow plate. C_{Df} and C_{Lf} are defined by:

$$(C_{Df}, C_{Lf}) = (\sqrt{D_f^2}, \sqrt{L_f^2}) / (0.5 \rho U^2 Wl) \tag{3}$$

Where, D_f is the fluctuating fluid force in the flow direction, and L_f the fluctuating fluid force in direction perpendicular to flow. The C_{Lf} of the snow plate of ①, located at the topmost part of the snow fence has the maximum value because this snow plate is

strongly influenced by the effect of the shear layer that rolls up from the upper end of the snow fence. The C_{Df} and C_{Lf} of the airfoil

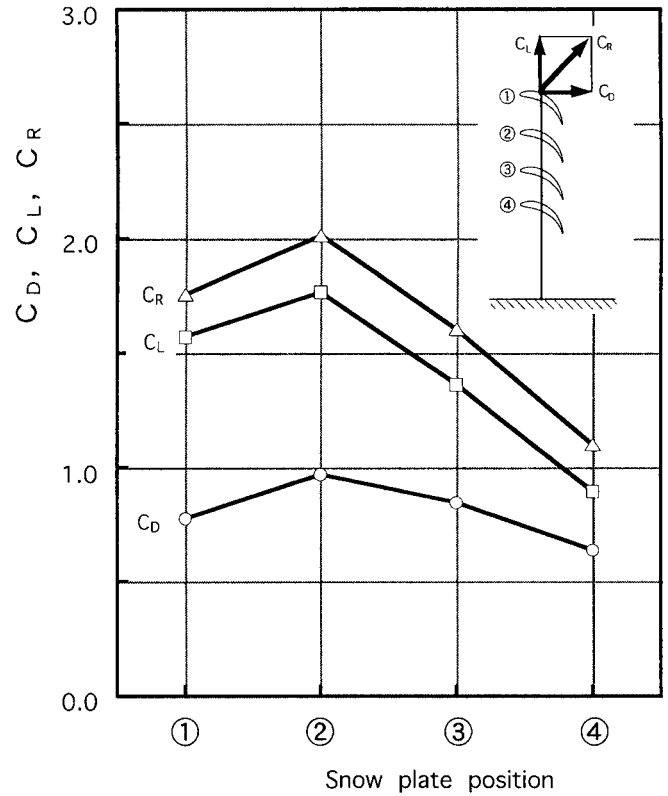


Fig. 6 C_D , C_L , and C_R of each snow plate

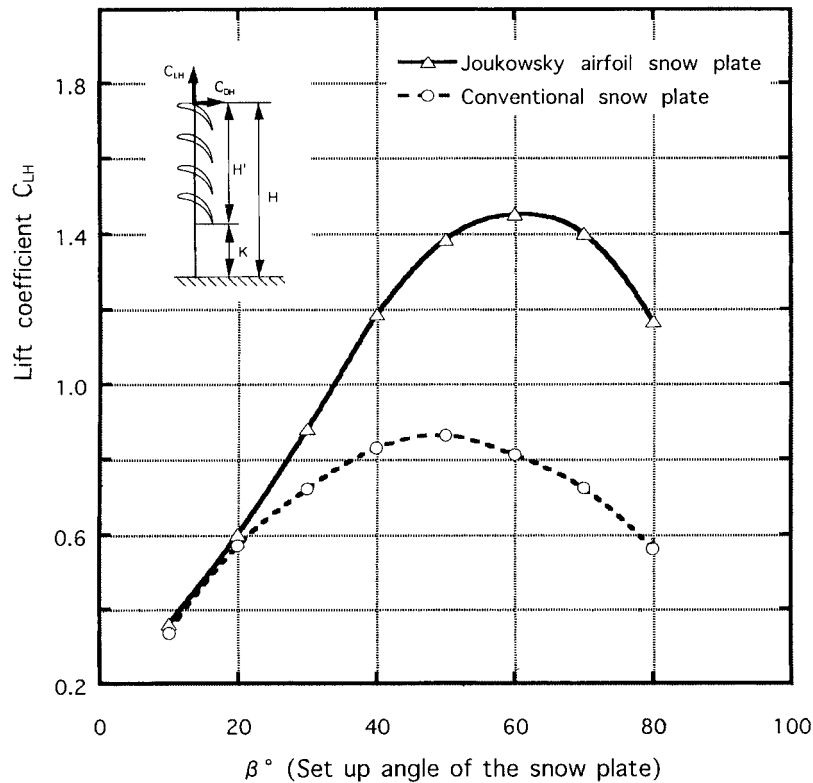


Fig. 5 Lift coefficient, C_{LH} , of the snow fence versus the set up angle, β

snow plates of ②, ③, and ④, however, are very small as compared to the airfoil snow plate of ① because the effect of the shear layer rolled-up from the upper end of the snow fence is weakened. To verify the generation mechanism of the fluctuating fluid forces, the power spectrum distributions of the fluctuating drag and lift acting on the airfoil snow plates and the fluctuating velocity at $x/H=2.0$ (the y direction position is changed) behind the snow fence were investigated. The respective findings are shown in figures 8 and 9. The fluctuating drag on and lift of the airfoil snow plates vary with a prevailing frequency of $f_p=19.9$ Hz, identical to that of the fluctuating velocity behind the snow fence. Fluctuating drag and lift therefore are generated by the rolling-up of the shear layer with periodicity from the upper end of the snow fence. The energy level of the power spectrum of the fluctuating drag and the lift of the snow plate of ① also are considerably larger than those of the other snow plates. Accordingly, generation of the fluctuating fluid forces on airfoil snow plates can be suppressed by controlling the shear layer because these forces occur as the result of

the rolling-up of the shear layer from the upper end of the snow fence.

3.3 Control of fluctuating fluid forces acting on the snow plate

The fluctuating drag and lift acting on the airfoil snow plates were suppressed by the use of a perforated plate attached to the topmost part of the snow fence, as shown in Fig.3. A flow visualization experiment was made in a water channel to determine the optimum value of porosity, a , of the perforated plate and interval, G , between the airfoil snow plate attached to the topmost part of the snow fence and the perforated plate. Figure 10 shows visualization of the flow pattern around the snow fence with a perforated plate attached to its topmost part. The Reynolds number, R_H , based on the height, H , of the snow fence and the approaching flow

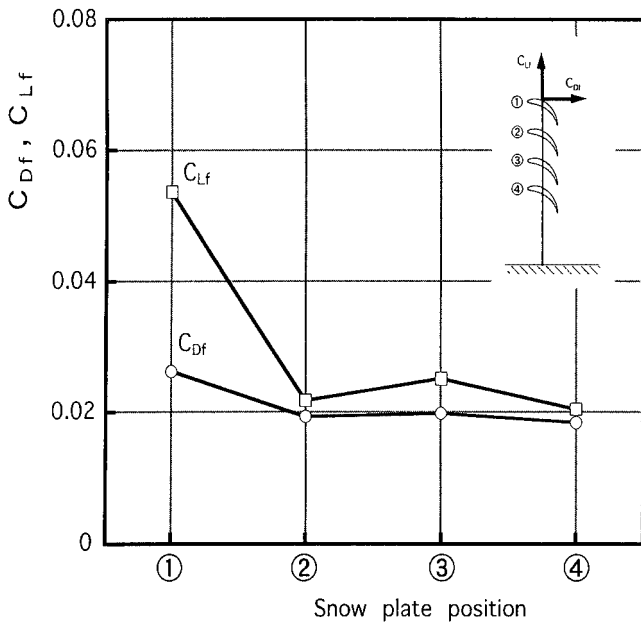


Fig. 7 C_{Df} and C_{Lf} of each snow plate

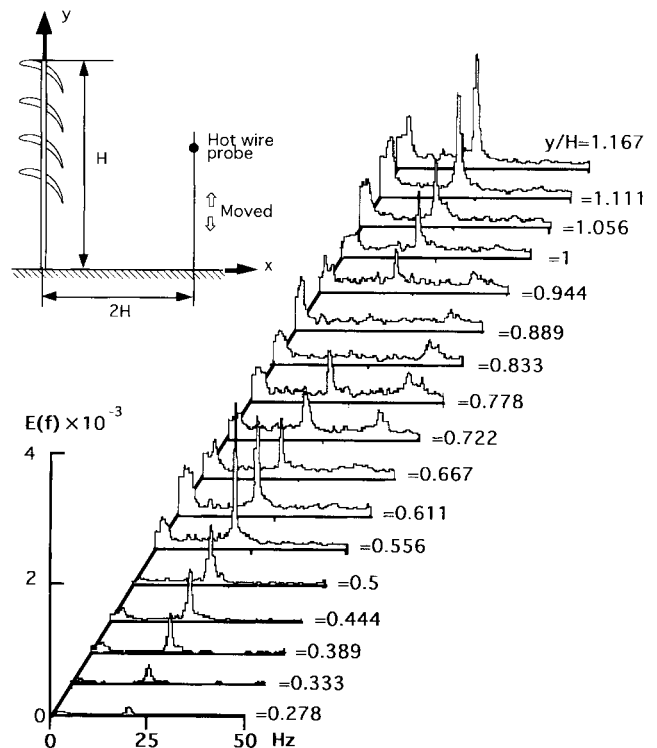


Fig. 9 Power spectrums of fluctuating velocity behind the snow fence

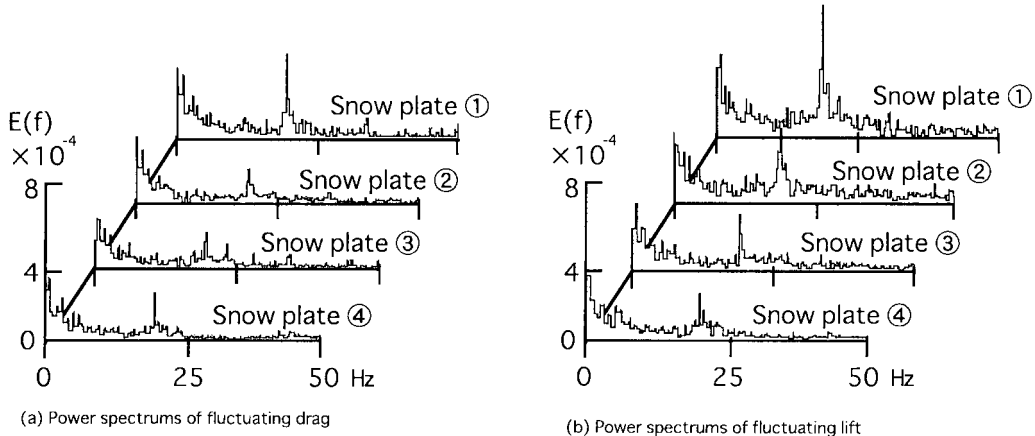


Fig. 8 Power spectrums of fluctuating drag and lift of the airfoil snow plates

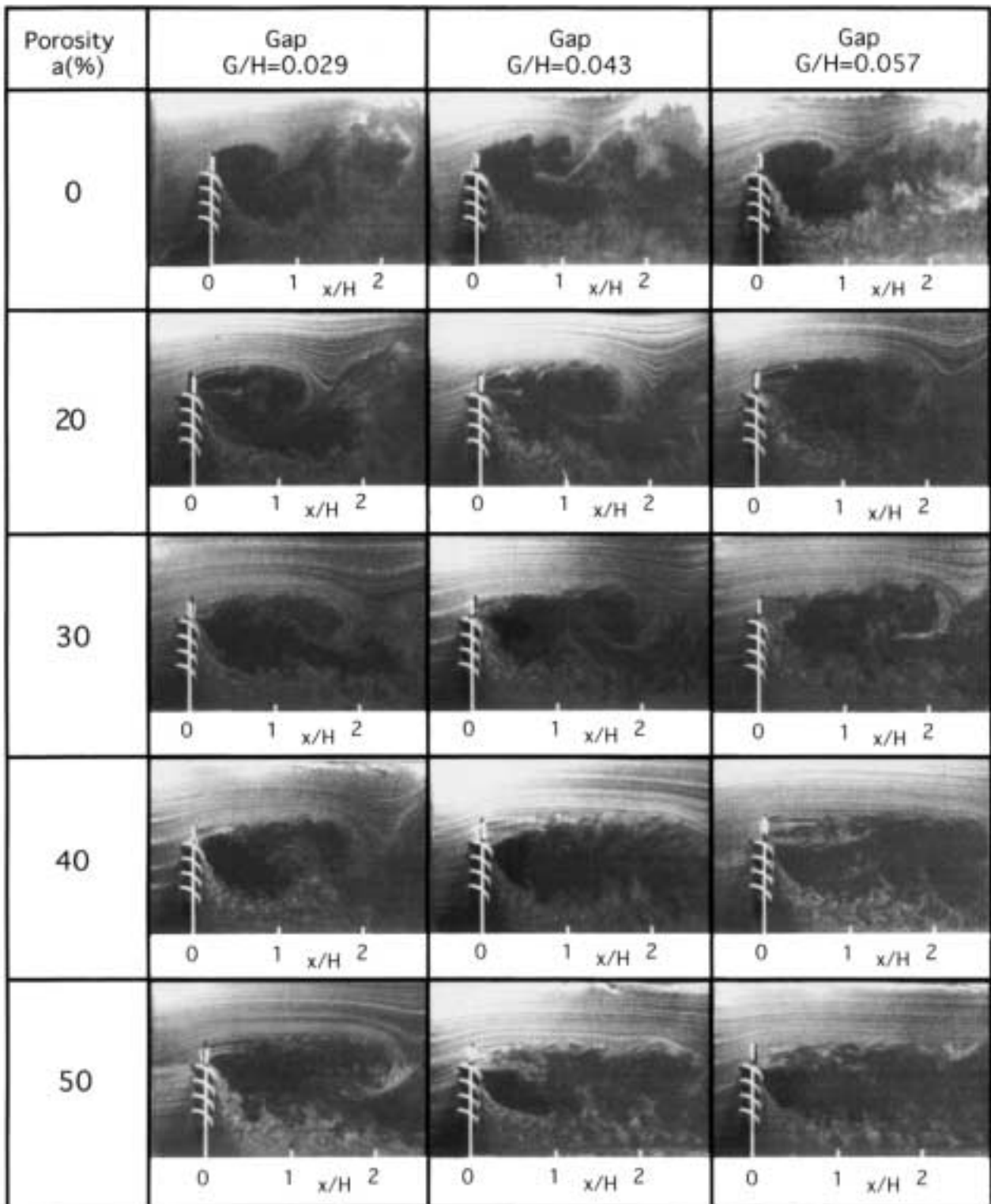


Fig. 10 Visualization of the flow pattern around the snow fence with a perforated plate attached to its topmost part

velocity, U , was 6.8×10^3 in this experiment, which value differs from $R_H=1.03 \times 10^5$ found in measuring the aerodynamic fluid forces in a wind tunnel, but there does not appear to be a problem in the case of a qualitative evaluation. The porosity of the perforated plate was changed (0%, 20%, 30%, 40%, and 50%), as was the G/H interval between the airfoil snow plate and perforated plate (0.029, 0.043, and 0.057). When the porosity of $a=0\%$, 20%, and 30%, the rolling-up of the shear layer that is separated from the topmost part of the snow fence occurs, whereas for porosities of 40% and 50% and an interval of $G/H=0.057$, almost no rolling-up of the shear layer occurs. Also, the flow through the bottom gap moves along the surface of road with no rolling-up for porosities of $a=40\%$ and 50% and on interval of $G/H=0.057$. Accordingly, a perforated plate at position $G/H=0.057$, and which has a porosity greater than 40% is judged to be the most effective

for suppressing the rolling-up of the shear layer that is separated from the topmost part of the snow fence.

Figure 11 shows the fluctuating drag, C_{Df} and fluctuating lift, C_{Lf} , coefficients of the airfoil snow plates for a perforated plate installation at the interval $G/H=0.057$ and with a porosity of 40%. The C_{Lf} and C_{Df} of the airfoil snow plate of ① are markedly reduced as compared to values without the perforated plate. The C_{Lf} and C_{Df} of the other airfoil snow plates also become small as compared to values without the perforated plate. Figure 12 shows the power spectrum of the fluctuating drag and fluctuating lift acting on the snow plates, and Figure 13 that of the fluctuating velocity behind the snow fence with a perforated plate having porosity of 40% and an interval $G/H=0.057$. No clear spectral peaks exist for fluctuating drag, fluctuating lift, and fluctuating velocity, evidence that the perforated plate is very effective in suppressing fluctuating fluid forces.

Figure 14 shows the time-averaged drag, C_D , and lift, C_L , coefficients of each airfoil snow plate for a perforated plate with a porosity of 40% and interval of $G/H=0.057$. Except for airfoil

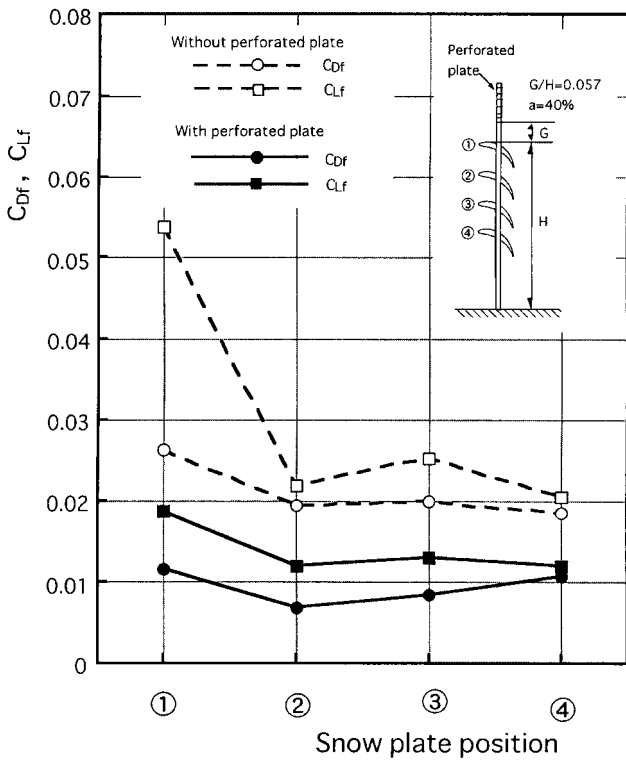


Fig. 11 C_{Df} and C_{Lf} of each snow plate when a perforated plate is attached to topmost part of the snow plate

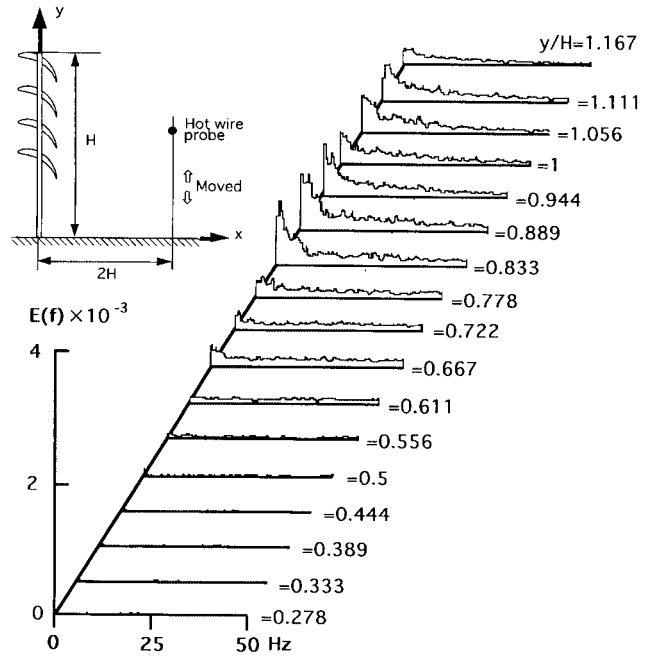
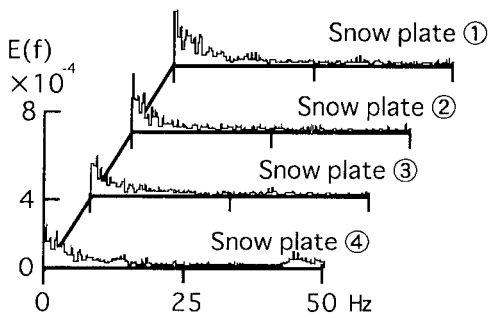
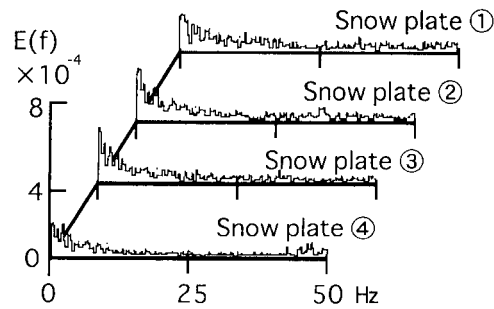


Fig. 13 Power spectrums of fluctuating velocity behind the snow fence (with perforated plate)



(a) Power spectrums of fluctuating drag



(b) Power spectrums of fluctuating lift

Fig. 12 Power spectrums of fluctuating drag and lift of the airfoil snow plates (with perforated plate)

snow plate ①, C_D and C_L are decreased as compared with snow plates without the perforated plate, the C_D and C_L of the airfoil snow plate of ① being considerably increased as compared with snow plates without the perforated plate. This is because the separation of the flow along the upper surface of the airfoil snow plate is suppressed as a result of deflection by the perforated plate, and

negative pressure on the upper surface is increased. Accordingly, this situation must be taken into account when evaluating the required strength of the airfoil snow plate of ①.

3.4 Vibration characteristics and suppression of the vibration of a snow plate

The response of the airfoil snow plates was measured by the use of the free-rotation vibration equipment shown in Fig.2. Figure 15 shows the response characteristics of each airfoil snow plate in the snow fence without a perforated plate. The ordinate

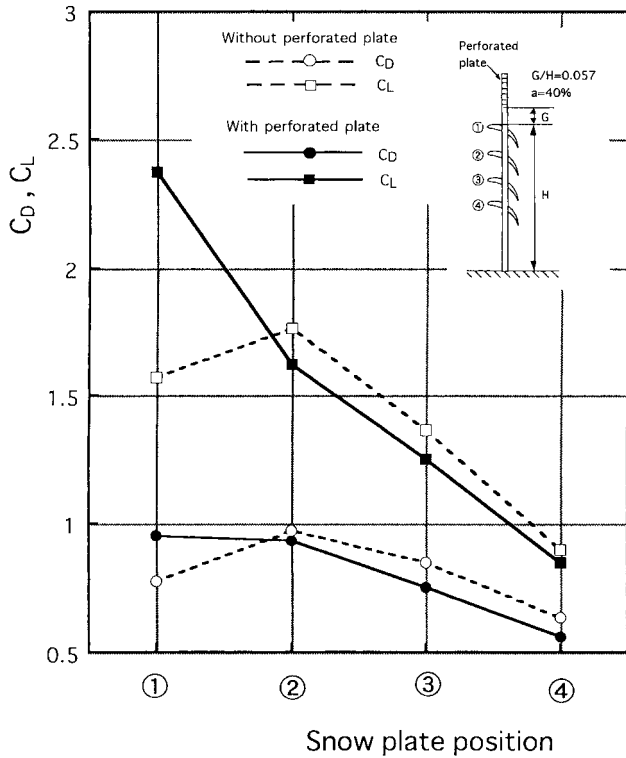


Fig. 14 C_D and C_L of each snow plate when a perforated plate is attached to topmost part of the snow plate

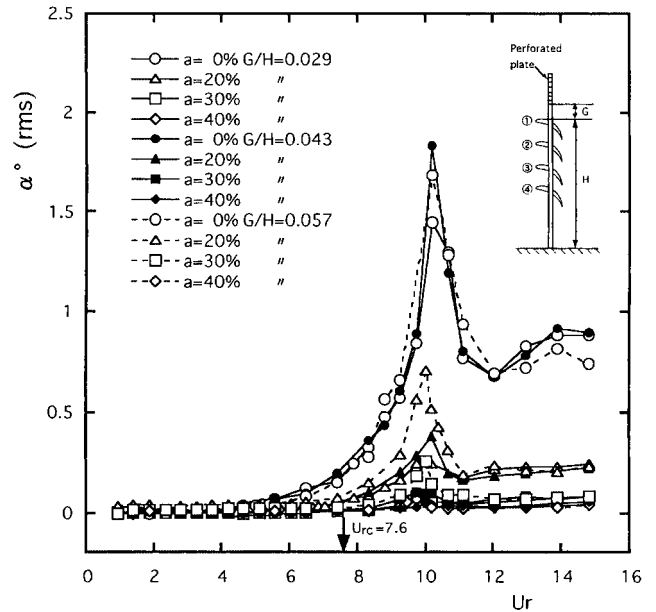


Fig. 16 Rotary oscillation response of snow plate number ① when a perforated plate is attached to the topmost part of the snow fence

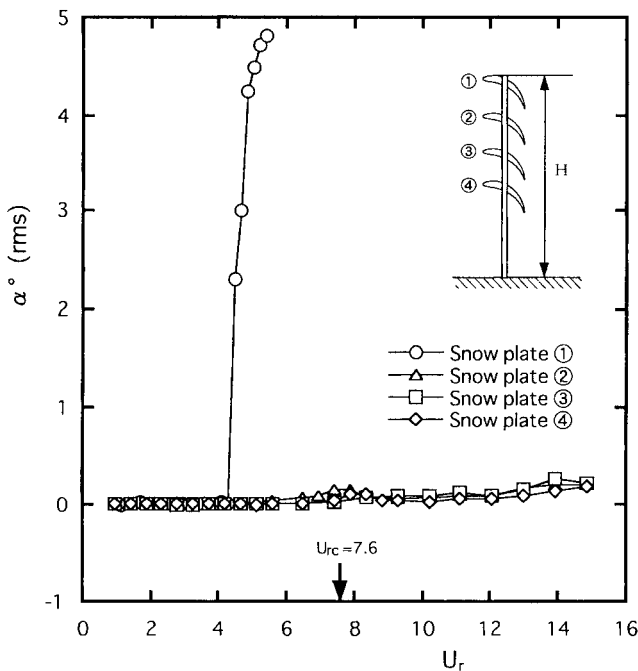


Fig. 15 Rotary oscillation response of each snow plate in the absence of a perforated plate

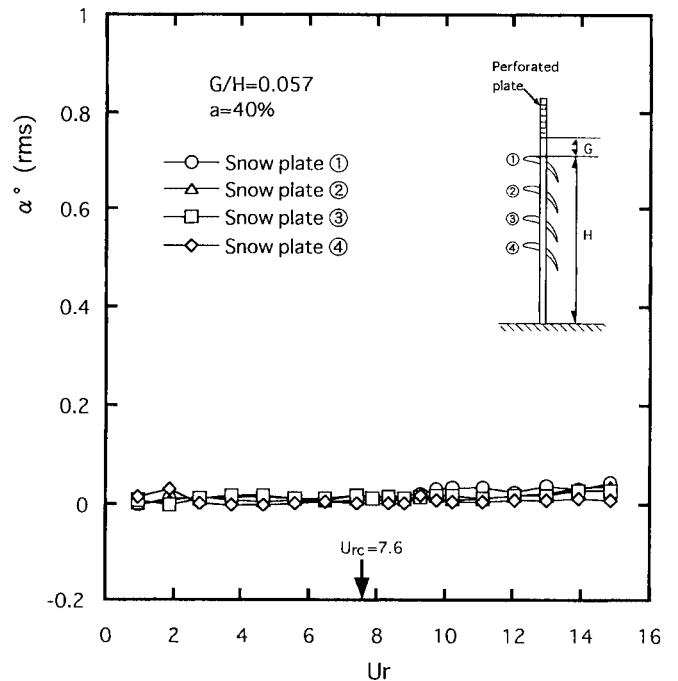


Fig. 17 Response of each snow plate when a perforated plate is attached to the topmost part of the snow fence

gives the rms value of the amplitude angle, a , of rotational oscillation. The abscissa gives the reduced velocity, U_r , [$=U/(f_c \cdot W)$]. Negligible the flow-induced vibration occurs at the airfoil snow plates ②, ③, and ④, whereas vibrations of the airfoil snow plate ① occur from approximately $U_r=4.0$ and are quickly amplified with the increase in the reduced velocity.

Figure 16 shows the response characteristics of the airfoil snow plate of ① when the perforated plate is installed in the topmost part of the snow fence. The porosity of the perforated plate was varied at 0%, 20%, 30%, and 40%, and the interval G/H at 0.029, 0.043, and 0.057. The rotational oscillation response decreases with the porosity of the perforated plate. Notably, the generation of flow-induced vibration is completely suppressed at the porosity of $a=40\%$ and interval of $G/H=0.057$. The generation of flow-induced vibration of the airfoil snow plate of ① therefore can be completely prevented by installing a perforated plate. Figure 17 shows the response characteristics of the airfoil snow plates for installation of a perforated plate of $a=40\%$ and $G/H=0.057$. No generation of flow-induced vibration was observed for either airfoil snow plate. These findings indicate that installation of a perforated plate is very effective in suppressing the generation of flow-induced vibration of airfoil snow plates.

3.5 Performance evaluation of the snow fence with a perforated plate

The snow fence that gave the best performance had a height of $H=2.8$ m, bottom gap of $K=1.2$ m, size of $W=650$ mm and setup angle of $\beta=60^\circ$ for Jowkowsky airfoil snow plate. Installation of the perforated plate at the topmost part of the snow fence is very effectively suppresses flow-induced vibration of the airfoil snow plates. Therefore, when a perforated plate is installed at the topmost part of such a snow fence the effectiveness of the fence for preventing blowing snow disasters was investigated. Figure 18 shows the spatial density distributions of blowing-snow around the snow fence for differences in the porosity of the perforated plate when the interval between the airfoil snow plate attached to the topmost part of the snow fence and perforated plate was constant at $G/H=0.057$. The density distribution of blowing-snow was measured in a blowing-snow wind tunnel. High-density, blowing snow passed to the vicinity of the road surface increases as porosity increases. For a porosity of $a=40\%$, most of the blowing-snow passes below half the driver's eye level of 1.35 m, and visibility is more greatly improved as compared with visibility without the perforated plate, evidence that the installation of a perforated plate therefore is a very effective method for improving visibility.

4. CONCLUSIONS

- (1) Time-averaged and fluctuating fluid forces acting on a snow fence and airfoil snow plates examined could evaluate of the required design strength.
- (2) Fluctuating fluid forces acting on airfoil snow plates, which are induced by the rolling-up of the shear layer separated from the topmost part of the snow fence, are the greatest on an airfoil snow plate installed at the topmost part of the snow fence.
- (3) Flow-induced vibration of the airfoil snow plate at the topmost part of the snow fence is generated and amplified by an increase in wind velocity.
- (4) A perforated plate installed at the topmost part of the snow fence is very effective for suppressing the fluctuating fluid forces that act on airfoil snow plates.
- (5) Flow-induced vibration of airfoil snow plates can be completely suppressed by the use of a perforated plate with porosity of $a=40\%$ and setup interval of $G/H=0.057$.
- (6) The blowing-off performance of a snow fence with the perforated plate is much better than that of a snow fence without such a plate.

ACKNOWLEDGMENTS

This study was supported by a Grant-in-Aid for Scientific Research [(B)(2) (No.09558048)] from the Ministry of Education, Science, Sports, and Culture of Japan.

REFERENCES

- Sakamoto, H., Haniu, H., Kiyota, M. and Obata, Y., 1992. Development and performance of snow fences for the prevention of blowing-snow disasters, Transactions of the Japan Society of Mechanical Engineers (B), 58; 550: 2017-2023. (in Japanese).
- Sakamoto, H., Moriya, M., Takai, K. and Obata, Y., 2000. Development of

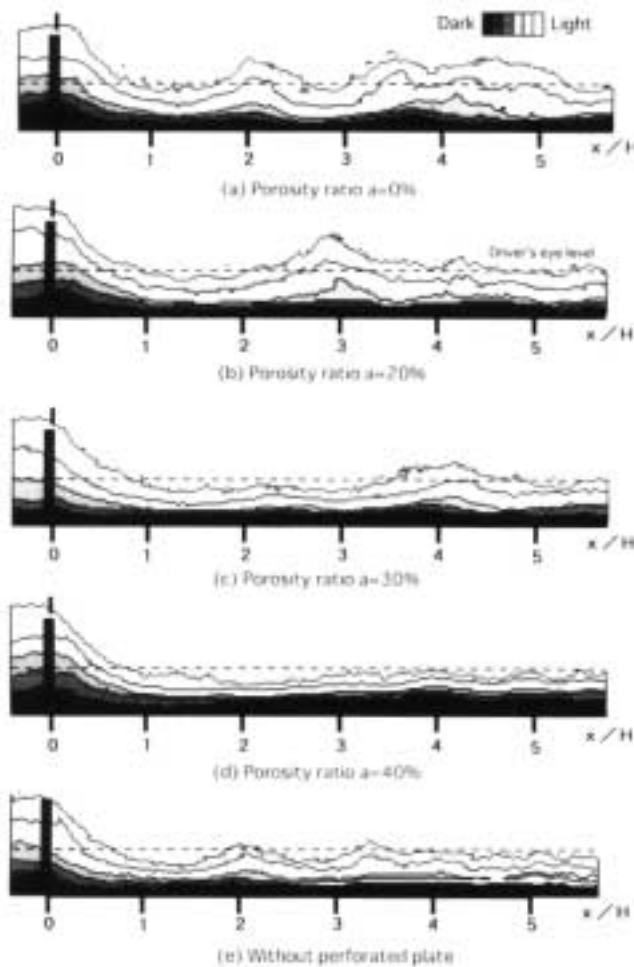


Fig. 18 Density distribution of blowing snow for the snow fence with a perforated plate

a new type snow fence with airfoil snow plates to prevent blowing-snow disasters (Part 1 Evaluation of performance by blowing-snow simulation in a wind tunnel), Journal of Natural Disaster Science.

So, R.M.C. and Savkar, S.D., 1981. Buffeting forces on rigid circular cylinders in cross flows, Journal of Fluid Mechanics, 105; 397-425.

NOMENCLATURE

A : projected area based on length of $H'=(H-K)$
 a : porosity of the perforated plate
 C_D : time-averaged drag coefficient of the airfoil snow plate
 C_{Df} : fluctuating drag coefficient of the airfoil snow plate
 C_{DH} : time-averaged drag coefficient of the snow fence
 C_L : time-averaged lift coefficient of the airfoil snow plate
 C_{Lf} : fluctuating lift coefficient of the airfoil snow plate
 C_{LH} : time-averaged lift coefficient of the snow fence
 C_R : time-averaged resultant force coefficient of the airfoil snow plate
 D : time-averaged drag acting on the airfoil snow plate

D_f : fluctuating drag acting on the airfoil snow plate
 D_H : time-averaged drag on the snow fence
 d : porous hole diameter of the perforated plate
 f_c : natural frequency of the airfoil snow plate
 f_v : frequency of vortex shedding from the airfoil snow plate
 G : interval between the airfoil snow plate and perforated plate
 H : height of the snow plate
 K : height of the bottom gap
 L : time-averaged lift of the airfoil snow plate
 L_f : fluctuating lift of the airfoil snow plate
 L_H : time-averaged lift of the snow fence
 l : span length of the airfoil snow plate
 U_r : reduced velocity
 U_{rc} : reduced velocity for vortex resonance
 w : width of the perforated plate
 α : rms value of amplitude angle